8-1-2015

Losartan Treatment Attenuates Tumor-induced Myocardial Dysfunction

Sarah C.W. Stevens
The Research Institute at Nationwide Children's Hospital

Markus Velten
The Research Institute at Nationwide Children's Hospital

Dane J. Youtz
The Research Institute at Nationwide Children's Hospital

Yvonne Clark
Ohio State University - Main Campus

Runfeng Jing
Ohio State University - Main Campus

See next page for additional authors

Accepted version. *Journal of Molecular and Cellular Cardiology*, Vol. 85 (August 2015): 37-47. DOI.

Authors
Sarah C.W. Stevens, Markus Velten, Dane J. Youtz, Yvonne Clark, Runfeng Jing, Peter J. Reiser, Sabahattin Bicer, Raymond D. Devine, Donna O. McCarthy, and Loren E. Wold

Losartan Treatment Attenuates Tumor-Induced Myocardial Dysfunction

Sarah CW Stevens
Center for Cardiovascular and Pulmonary Research, The Research Institute at Nationwide Children's Hospital, Columbus, OH
Markus Velten
Department of Anesthesiology and Intensive Care Medicine, Rheinische Friedrich-Wilhelms-University, University Medical Center, Bonn, Germany
Dane J. Youtz
Center for Cardiovascular and Pulmonary Research, The Research Institute at Nationwide Children's Hospital, Columbus, OH
Yvonne Clark
College of Nursing, The Ohio State University, Columbus, OH
Runfeng Jing
College of Nursing, The Ohio State University, Columbus, OH

Journal of Molecular and Cellular Cardiology, Vol 85 (August 2015): pg. 37-47. DOI.

Peter J. Reiser

Division of Biosciences, College of Dentistry, The Ohio State University, Columbus, OH

Sabahattin Bicer

Division of Biosciences, College of Dentistry, The Ohio State University, Columbus, OH

Raymond Devine

Molecular, Cellular and Developmental Biology Graduate Program, The Ohio State University, Columbus, OH

Donna O. McCarthy

College of Nursing, The Ohio State University, Columbus, OH

College of Nursing, Marquette University, Milwaukee, WI

Loren E. Wold

Center for Cardiovascular and Pulmonary Research, The Research Institute at Nationwide Children's Hospital, College of Nursing, The Ohio State University, Dorothy M. Davis Heart and Lung Research Institute and Department of Physiology and Cell Biology, College of Medicine, The Ohio State University, Columbus, OH

Abstract: Fatigue and muscle wasting are common symptoms experienced by cancer patients. Data from animal models demonstrate that angiotensin is involved in tumor-induced muscle wasting, and that tumor growth can independently affect myocardial function, which could contribute to fatigue in cancer patients. In clinical studies, inhibitors of angiotensin converting enzyme (ACE) can prevent the development of chemotherapy-induced cardiovascular dysfunction, suggesting a mechanistic role for the renin-angiotensin-aldosterone system (RAAS). In the present study, we

Journal of Molecular and Cellular Cardiology, Vol 85 (August 2015): pg. 37-47. DOI.

investigated whether an angiotensin (AT)1-receptor antagonist could prevent the development of tumor-associated myocardial dysfunction. Methods and Results: Colon26 adenocarcinoma (c26) cells were implanted into female CD2F1 mice at 8 weeks of age. Simultaneously, mice were administered Losartan (10 mg/kg) daily via their drinking water. In vivo echocardiography, blood pressure, in vitro cardiomyocyte function, cell proliferation assays, and measures of systemic inflammation and myocardial protein degradation were performed 19 days following tumor cell injection. Losartan treatment prevented tumor-induced loss of muscle mass and in vitro c26 cell proliferation, decreased tumor weight, and attenuated myocardial expression of interleukin-6. Furthermore, Losartan treatment mitigated tumor-associated alterations in calcium signaling in cardiomyocytes, which was associated with improved myocyte contraction velocity, systolic function, and blood pressures in the hearts of tumor-bearing mice. Conclusions: These data suggest that Losartan may mitigate tumor-induced myocardial dysfunction and inflammation.

Keywords: cancer cachexia, cardiovascular function, calcium signaling, Losartan, cardiomyocyte

Introduction

Cancer cachexia, a syndrome consisting of fatigue, muscle wasting, and weight loss with or without anorexia, is observed in a large percentage of cancer patients with incurable disease[1] and contributes to 22 percent of cancer deaths.[1,2] New research by our lab and others has shown that cancer cachexia involves not only the loss of skeletal muscle, but can also cause pathologic alterations within the heart.[2,3] The resultant effects on myocardial function likely contribute to fatigue and decreased quality of life in these patients.

We and others have demonstrated tumor-induced cardiac remodeling and myocardial dysfunction.[2–4] Tumor-induced cardiac remodeling involves increased expression of pro-inflammatory cytokines, such as interleukin-6 (IL-6).[5] as well as ventricular wall thinning and decreased troponin I levels (a protein involved in cardiac contraction).[2] Previous work from our lab has also shown increased expression of MAFbx mRNA, a muscle-specific ubiquitin ligase involved in the ubiquitin proteasome pathway (UPP) of protein degradation, and Bnip3, a protein involved in the formation of autophagic vesicles, in mouse hearts inoculated with the colon26 (c26) adenocarcinoma cell line [3]. We also recently showed that IL-6 levels are elevated in both the serum and heart muscle in this model.[3] Together, these results

indicate an increase in muscle protein degradation and inflammation in the heart, and myocardial dysfunction due to growth of the c26 adenocarcinoma.

Current data regarding the impact of the renin-angiotensin-aldosterone system (RAAS) on the development of cancer-induced myocardial dysfunction and its potential therapeutic properties are inconclusive. Angiotensin II receptor subtypes 1 and 2 (AT_1 and $_2$) have direct effects on tumor development through the induction of cell proliferation and vascular endothelial growth factor (VEGF)-induced angiogenesis.[6] Furthermore, the AT_2 receptor antagonist Losartan has been shown to limit tumor-associated angiogenesis, inhibit collagen synthesis, and attenuate tumor progression. Additionally, Losartan improves the distribution and efficacy of nanotherapeutics in tumor therapy.[7] Recently, a clinical trial revealed that treatment with a high dose of the ACE inhibitor Enalapril and also beta-receptor blocker treatment with Carvedilol prevented the development of chemotherapeutic-induced myocardial dysfunction.[8] These studies suggest a mechanistic role for the RAAS in cancer treatment-induced myocardial dysfunction.[9] Experimental studies reported preventative effects of beta-blockers and aldosterone antagonists but not angiotensin-converting-enzyme (ACE) inhibitors on loss of body weight and skeletal muscle mass, as well as tumor-induced alterations in cardiac dimensions in a mouse model of liver cancer-induced cardiac cachexia and muscle wasting.[10] More recent studies indicated that combined treatments of chemotherapeutics with AT_1 receptor antagonists improved survival.[11] However, few studies have investigated the role of the RAAS in the direct effects of tumor progression and subsequent myocardial dysfunction and potential therapeutic prospects.

The RAAS is known to play a major role in myocardial remodeling and dysfunction. Recently, Angiotensin II (AngII) has been implicated in skeletal muscle catabolism in tumor-bearing animals via activation of the UPP of myosin protein degradation. These data suggest that the RAAS could play a role in tumor-induced myocardial dysfunction.[12–17] In order to examine the impact of the RAAS in tumor-induced myocardial dysfunction and potential therapeutic feasibility, we treated c26 tumor-bearing mice with Losartan (LOS), an AT_1 antagonist, and examined *in vivo* and *in vitro* myocardial function,

blood pressures, and AngII serum concentration following cancer cachexia development.

Materials and Methods

Animal Model

Animal protocols were approved by the Institutional Care and Use Committee (IACUC) at the Research Institute at Nationwide Children's Hospital and The Ohio State University. One hundred adult (8 week old) female CD2F1 mice (Harlan) were handled in accordance with NIH guidelines and housed in a specific pathogen free facility, five per cage on a 12 hour light/dark cycle. Half of the mice were inoculated with c26 tumor cells (tumor) and half injected with a similar saline volume served as healthy controls (control). The c26 cells were cultured and injected subcutaneously above the scapula, as previously described.[3] Half of the tumor (tumor/LOS) and half of the control (control/LOS) mice were administered 10 mg/kg of Losartan (LOS) daily via their drinking water, beginning on the day of tumor cell injection.

Animals were euthanized on day 19 after tumor cell injection via pentobarbital injection (20mg/kg for myocyte isolation) or carbon dioxide inhalation followed by cervical dislocation for tissue collection as approved by the American Veterinary Medicine Association Panel on Euthanasia. Hearts were removed, weighed and then used for primary cardiomyocyte isolation or snap-frozen in liquid nitrogen for molecular analyses. Gastrocnemius muscles and tumors were removed, weighed, and snap-frozen in liquid nitrogen.

Real-time Polymerase Chain Reaction

Total RNA was extracted from 100 mg cardiac tissue as previously described.[3] Real time PCR (RT-PCR) for MAFbx (Forward 5'-GTGCTTACAACTGAACATATGCA-3'; Reverse 5'-TGGCCCAGGCTGACCA-3'), GAPDH (Forward 5'-ATGGTCAAGGTCGGTGTGAACGG-3'; Reverse 5'-AGGGGTGGTTGATGGCAACAATCT-3') and IL-6 (Forward 5'-GCCAGAGTCCTTCAGAGAGATACAGAAACTC-3'; Reverse 5'-AGCCACTCCTTCTGTGACTCCAGCTTA-3') was performed using primer

pairs and SYBR super mix (BioRad). The TaqMan Gene Expression Assay was used to detect gene expression of Bnip3 according to the manufacturer's instructions. Briefly, 25 µl samples were run in duplicate in an iCycler iQ5 (BioRad) for 40 cycles at 95°C for 15 seconds and 60°C for 1 minute after the initial 10 minute 95°C denaturation period. MAFbx, Bnip3, and IL-6 levels were all normalized to GAPDH expression.[3]

Plasma Cytokines

Plasma was obtained from mice using an abdominal aortic stick immediately following euthanasia. Blood was collected in EDTA tubes and centrifuged at 1500 x g, 10 min, 4°C to separate the plasma. Plasma levels of interleukin (IL)-1, IL-6, IL-10, IL-12, interferon-gamma (IFN-γ), tumor necrosis factor-α (TNF-α), and chemokine (C-X-C motif) ligand 1 (CXCL1) were measured using the MSD Mouse Pro-inflammatory 7-Plex Ultra-Sensitive Kit (Meso Scale Discovery K15012C) according to the manufacturer's instructions.

Echocardiography

On day 19 post-injection, *in vivo* cardiac function was assessed in 56 mice (15 control, 14 control/LOS, 17 tumor, and 10 tumor/LOS) via echocardiography using a VisualSonics Vevo 2100 Ultra High Resolution In Vivo Imaging System (VisualSonics, Toronto, ON, Canada) as previously described.[3,18] Briefly, mice were anesthetized with 1.5% isofluorane in an anesthesia induction chamber. Following the induction of anesthesia, mice were placed on a warming pad, and connected to a three lead electrocardiogram monitor. During echocardiographic analyses, mice were continuously sedated with 1.0% isoflurane (in 100% O_2) to receive identical anesthetic conditions for all groups. Left ventricular systolic diameter ($LVES_d$), left ventricular diastolic diameter ($LVED_d$) and left ventricular posterior wall thickness at systole (PWT_s) and diastole (PWT_d) were measured using the M-mode echocardiogram. Fractional shortening (FS) was calculated using $FS=(LVED_d-LVES_d)/LVED_d*100$. Ejection fraction (EF) was calculated using the following equation: $EF=(LVED_d-LVES_d/LVED_d)*100$. Stroke volume (SV) was calculated using the Doppler flow Velocity-Time Integral (VTI) at the LV outflow tract

(LVOT) and the aortic diameter (Ao), ($LVOT^2$ * 0.785 * Ao VTI). LV mass was calculated using the equation (left ventricular anterior wall (LVAW)+$LVED_d$+ PWT_d)^3-($LVED_d$)^3.[19]

Ventricular Myocyte Isolation and Functional Assessment

Following echocardiography, cardiomyocytes were isolated as previously described[3,18,20–23] Briefly, the hearts were removed and retrograde perfusion was performed with buffer, followed by 0.25 mg/ml Liberase DH (Roche), 0.14 mg/ml 2.5% Trypsin (Gibco) and 12.5 μM $CaCl_2$ for 5–7 minutes. Cells were dissociated by repeated pipetting and then filtered to remove cellular debris. Cardiomyocytes were exposed to increasing concentrations of $CaCl_2$ (to minimize the calcium paradox) and then plated on laminin-coated glass chambers.

Cardiomyocyte sarcomere function was examined using the Soft Edge MyoCam system (IonOptix Corporation), as previously described.[3,18,20–23] Only myocytes with normal sarcomeric appearance (absence of sarcomeric blebs) were used in these experiments. Peak shortening (sarcomere BL% peak height; cellular equivalent of %FS), time to 90 percent of peak shortening (TPS90), time to 90 percent relengthening (TR 90), and velocities of shortening (-dL/dt) and relengthening (+dL/dt) were measured following stimulation at 1 Hz.

Assessment of Cardiomyocyte Calcium Signaling

Ca^{2+} transients and caffeine-induced Ca^{2+} release were measured in isolated myocytes loaded with fura-2 AM, as previously described.[3,18,20–23] Briefly, myocytes were incubated with 0.5 μM fura-2 AM for 10 minutes and fluorescence was recorded using the Ionoptix dual-excitation fluorescence photomultiplier system through a 40x oil immersion objective. Fluorescence was achieved by excitation at 360 nm, followed by 380 nm, and emission was detected between 480–520 nm. For Ca^{2+} transient measurements, cells were stimulated at 0.5 Hz and changes in cytosolic Ca^{2+} levels were inferred from the ratio of fluorescence intensity at the two wavelengths. Caffeine-induced Ca^{2+} release from the SR was assessed in fura-2AM loaded cells by rapidly applying 20 mM caffeine and recording the resulting transient.

Integration under the resulting caffeine-induced Ca^{2+} release curve was calculated as an index of SR Ca^{2+} concentration.

Calcium sparks were measured by loading isolated cardiomyocytes with 20 μM Fluo-3 AM and 5% pluronic acid in Tyrode's Solution, which contained, in mM: 140 NaCl, 4 KCl,, 2 $CaCl_2$, 1 $MgCl_2$, 10 glucose, and 10 HEPES; pH 7.4 with NaOH. Cells were imaged using an inverted Zeiss 710 confocal microscope.[24]

GSSG/GSH Assay

The ratio of oxidized-to-reduced glutathione (GSSG/GSH) in left ventricular homogenates in all groups was measured as previously described,[25] as a global measure of antioxidant status in the heart.

Blood Pressure Measurements

Blood pressures were measured at baseline (prior to tumor/control injection), 12, and 18 days post injection using a computerized tail cuff system (BP-2000 Series II Visitech System Inc., Apex, North Carolina) as described previously.[18] Mice were trained before the procedure for 5 consecutive days to avoid anxiety during the procedure. In order to minimize procedure-induced effects, measurements were separated by 20 seconds to restore blood flow through the tail and preliminary assessments were not used for analyses. Ten values were recorded and averaged for analyses of the data from each mouse.

Angiotensin II Immunoassay

Blood was collected 18 days following tumor cell or sham injection and the serum was separated using Microtainer Serum Separator Tubes (BD, Franklin Lakes, NJ). Angiotensin II concentrations were assessed using a Fluorescent Immunoassay (Phoenix Pharmaceuticals, Inc. Burlingame, CA). According to the manufacturer's instructions, serum and primary antibody were incubated on a pre-coated fluorescent plate at 4°C overnight. Subsequently, a biotinylated Angiotensin-II peptide was added and allowed to incubate for 1.5 hours at room temperature. After washing,

samples were incubated with a Streptavidin-horseradish peroxidase conjugate (SA-HRP) for 1 hour at room temperature before the substrate was added and the reaction proceeded for 20 minutes before the relative fluorescence was determined using a fluorescent plate reader at an excitation and emission maxima of 325 and 420 nm respectively. Results were obtained by comparing the optical density to a standard series using 4-parameter logistic curve fitting software.

Colon26 (c26) Adenocarcinoma Cell Proliferation Assay

The effects of Losartan on c26 Adenocarcinoma cell proliferation were determined using a Tryptan blue assay. Cells were seeded at the same density onto separate plates and allowed to adhere overnight. The following day, either 1 mM or 10 mM of Losartan was added to the cells as previously described.[26] Once the control cells reached confluence, the media was removed and the cells were trypsinized, centrifuged and re-suspended in DPBS. Cells were mixed together with Trypan blue and viable cells were counted on an Improved Neubauer Hemocytometer and expressed as cells/mL.

Statistical Analyses

Data were analyzed using a two-way ANOVA to uncover main effects of tumor and drug treatment and interaction effect of tumor and drug treatment on outcome measures, followed by Bonferroni post-hoc testing to uncover specific group differences. For blood pressure measurements, the mean of five measures was used for statistical analyses. Statistical significance was set at $p<0.05$. Data are reported as mean ± standard error of the mean (SEM).

Results

Losartan treatment prevented tumor-related muscle wasting and reduced tumor progression

Body weights, excluding tumor weights, were assessed on day 19 and not different between tumor/sham and control/sham or tumor/LOS and control/LOS treated mice. However, tumor/LOS treated mice had lower body weights compared to control/sham

treated mice and statistical analyses indicated that Losartan treatment had a significant effect ($p<0.05$) on body weight (Table 1). Relative gastrocnemius weights were significantly lower in tumor/sham mice compared to control/sham mice. However, gastrocnemius weights were not different between tumor/LOS and control/LOS treated mice. Statistical analyses indicated that tumor cell injection significantly reduced gastrocnemius muscle weight relative to body weight ($p<0.05$), with no effect of Losartan treatment ($p=.06$) on relative gastrocnemius weights (Table 1). These data suggest that Losartan mitigated muscle wasting in the tumor-bearing mice. Heart weights were not different between groups and neither tumor growth nor Losartan treatment had an effect on relative heart weight (Table 1). Tumor weights were significantly lower in tumor/LOS mice compared to tumor mice ($p=.01$), suggesting that Losartan treatment significantly reduced tumor growth.

Table 1. Normalized body weight (exclusive of tumor weight), heart weight, gastrocnemius weight and tumor weight in mice. Normalized gastrocnemius and heart weight was calculated by dividing the measured tissue weight by the body weight. Data were analyzed using two-way ANOVA (tumor growth, Losartan treatment) and Bonferroni post hoc tests. Tumor weights were analyzed using student's t test.

	Body weight (excl. tumor weight) (g)	**Gastrocnemius weight (rel.) (mg/g)**	**Gastrocnemius weight (abs.) (g)**	**Heart weight (rel.) (mg/g)**	**Heart weight (abs.) (mg)**	**Tumor weight (g)**
control/sham (n=25)	21.4±0.4	4.76±0.2	9.88±0.24	6.27±0.27	133±2	N/A
tumor/sham (n=26)	19.6±0.4	4.22±0.2*	7.85±0.34*	6.87±0.37	132±2	1.26±0.1
control/LOS (n=20)	20.7±0.4	4.89±0.6	9.69±0.37	6.22±0.3	128±2	N/A
tumor/LOS (n=17)	18.4±0.6*	4.91±0.2	8,36±0.27*	6.63±0.5	118±2	0.88±0.1*

*$p<0.05$ compared to respective control.

Tumor-related cardiac degradation and inflammation is attenuated by Losartan treatment

Cardiac MAFbx, Bnip3, and IL-6 mRNA expression were significantly increased in tumor/sham compared to control/sham mice. However, cardiac MAFbx and Bnip3 mRNA expressions were not increased in tumor/LOS treated mice compared to control/LOS and

control/sham treated mice. IL-6 expression was not significantly different in tumor/LOS compared to control/LOS mice, but it was significantly lower than in tumor/control mice. Statistical analyses indicated effects of tumor cell injection on cardiac MAFbx ($p<.001$), Bnip3 ($p=.01$), and IL-6 ($p<.001$) mRNA expression. Losartan treatment had a significant effect on IL-6 mRNA expression ($p<.05$) alone, indicating that Losartan reduced expression of IL-6 mRNA in the hearts of both tumor-bearing and control mice (Figures 1A–C).

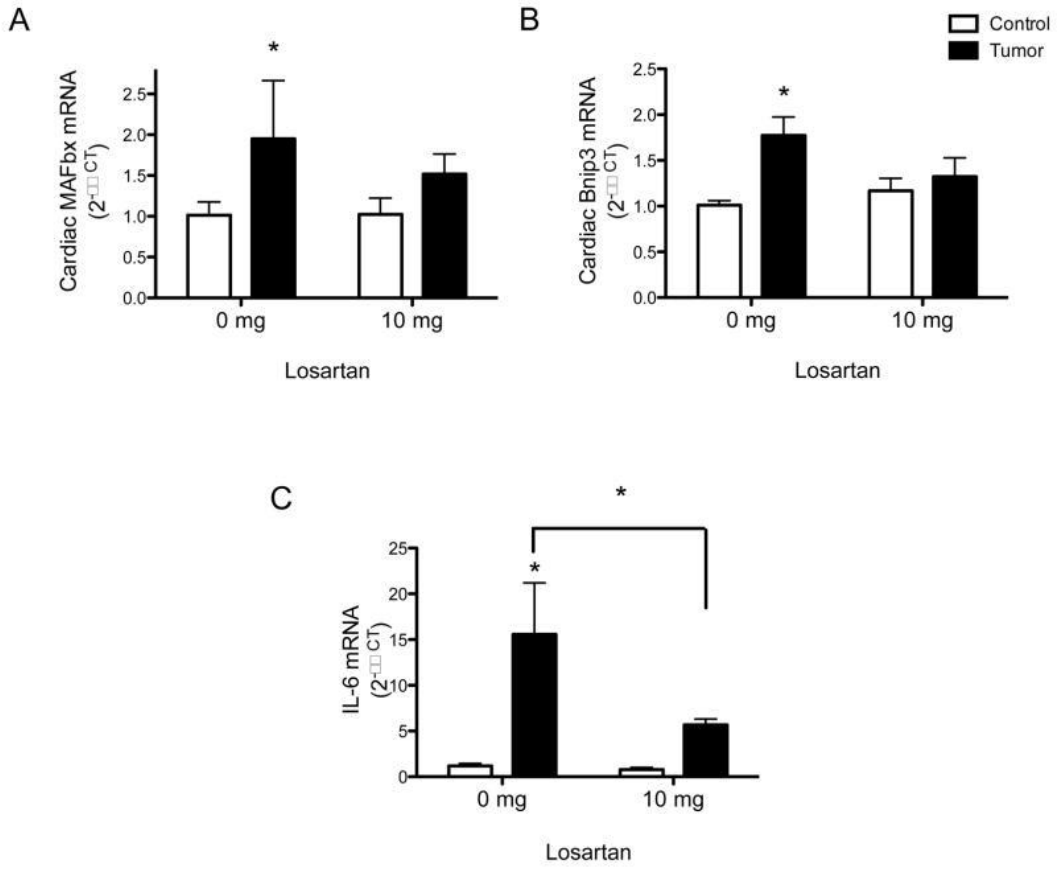

Figure 1. Gene expression of MAFbx (A), Bnip3 (B) and IL-6 (C) in cardiac tissue of tumor-bearing and Losartan-treated mice. Gene expression levels were determined using RT-PCR and are normalized to GAPDH expression. A, MAFbx, an indicator of ubiquitin proteasome function; B, Bnip3, an indicator of cellular autophagy; C, IL-6, an inflammatory cytokine. Data were analyzed using two-way ANOVA and Bonferroni post hoc pairwise comparisons. * $p<0.05$ compared to respective control. n=6 control/sham, n=5 tumor/sham, n=6 control/LOS, n=7 tumor/LOS.

Losartan treatment attenuated tumor-associated increases in plasma cytokine levels

IL-6 and CXCL1 protein concentrations were significantly increased in tumor/sham and tumor/LOS compared to respective controls (Figures 2A&B). IL-10 protein concentrations were increased in tumor/sham compared to control/sham but not in tumor/LOS compared to control/LOS treated mice (Figure 2C). Statistical analyses revealed an effect of tumor cell injection on plasma levels of IL-6 ($p<.0001$), CXCL1 (0.0001), IL-10 ($p<0.01$), and IL1-β ($p<0.05$) (Figures 2A–D) and an effect of Losartan treatment on plasma TNF-α levels ($p<0.05$) (Figure 2E). Neither tumor cell injection nor Losartan treatment affected plasma levels of IFN-γ (Figure 2F).

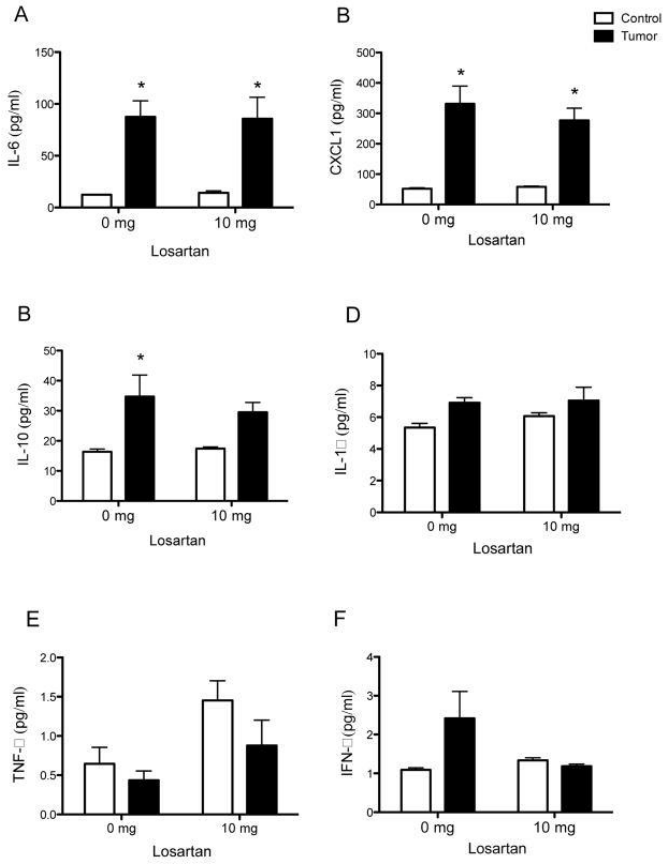

Figure 2. Plasma pro-inflammatory cytokine levels in tumor-bearing and Losartan-treated mice. Cytokine levels were determined using the Pro-inflammatory 7-Plex Ultra-Sensitive Kit. Data were analyzed using two-way ANOVA (tumor growth and Losartan treatment) and Bonferroni post hoc pairwise comparisons. * $p<0.05$ compared to respective control, n=10.

Journal of Molecular and Cellular Cardiology, Vol 85 (August 2015): pg. 37-47. DOI.

Losartan treatment prevented tumor-associated changes in LV dimensions and preserved myocardial function

Tumor cell injection reduced fractional shortening (FS), ejection fraction (EF), stroke volume (SV), posterior wall thickness in diastole (PWT_d), and systole (PWT_s) and increased systolic left ventricular dimension ($LVED_s$) in tumor/sham mice compared to control/sham mice. Losartan treatment prevented tumor-associated alterations in left ventricular dimensions and function. EF, EF, SV, PWT_d, PWT_s, were significantly greater and $LVED_d$, and $LVED_s$ significantly lower in tumor/LOS treated mice compared to tumor/sham mice. There were no differences between control/LOS and tumor/LOS treated mice. Heart rates were not different between groups. Statistical analyses indicated effects of tumor cell injection, Losartan treatment, and an interaction effect on $LVED_s$ ($p<0.001$), PWTs ($p<0.05$), SV ($p<0.01$), EF ($p<0.0001$), and FS($p<0.0001$) (Table 2). These results indicate that tumor cell injection reduced cardiac wall diameter and myocardial contractility, with Losartan treatment mitigating the effects of tumor cell injection on cardiac diameter and myocardial function.

Table 2. In vivo echocardiographic parameters in tumor-bearing and Losartan-treated mice. Fractional shortening (FS), ejection fraction (EF), left ventricular end diastolic diameter ($LVED_d$), left ventricular end systolic diameter ($LVES_d$), posterior wall thickness during diastole (PWT_d), posterior wall thickness during systole (PWT_s) and stroke volume (SV) in tumor-bearing and LOS-treated animals. Values were calculated from m-mode electrocardiograms as shown in Figure 3. Data were analyzed using two-way ANOVA (tumor growth and Losartan treatment) and Bonferroni post hoc tests.

	control/sham (n=15)	**tumor/sham (n=17)**	**control/LOS (n=14)**	**tumor/LOS (n=10)**
FS (%)	37.6±1.1	23.0±0.85*	38.5±0.9#	35.9±0.5#
EF	68.2±1.4	46.4±1.4*	68.8±1.1#	66.0±0.8#
$LVED_d$ (mm)	3.87±0.1	4.18±0.1	3.96±1.9	3.98±0.1
$LVED_s$ (mm)	2.45±0.1	3.21±0.1*	2.47±0.1#	2.55±0.1#
PWT_d (mm)	0.77±0.3	0.63±0.01*	0.74±0.03#	0.71±0.03
PWT_s (mm)	1.10±0.04	0.88±0.02*	1.14±0.03#	1.06±0.03#
SV (µl)	35.0±1.9	24.4±0.8*	36.0±1.7#	38.9±1.5#
HR (BPM)	455±11	460±12	449±8	442±9
LV mass (mg)	93.25±5.48	83.80±2.94	104.08±7.91	93.10±5.67

*$p<0.05$ compared to respective control,
#$p<0.05$ compared to tumor/sham.

Furthermore, there was an effect of tumor cell injection ($p<.001$) and an interaction effect ($p<0.05$) of tumor cell injection and Losartan treatment on PWT_d.; post hoc analyses revealed no significant differences between tumor/LOS and either group of control mice, suggesting that Losartan mitigated the effects of tumor cell injection. However, neither tumor cell injection nor Losartan treatment affected $LVED_d$ (Figure 3, Table 2).

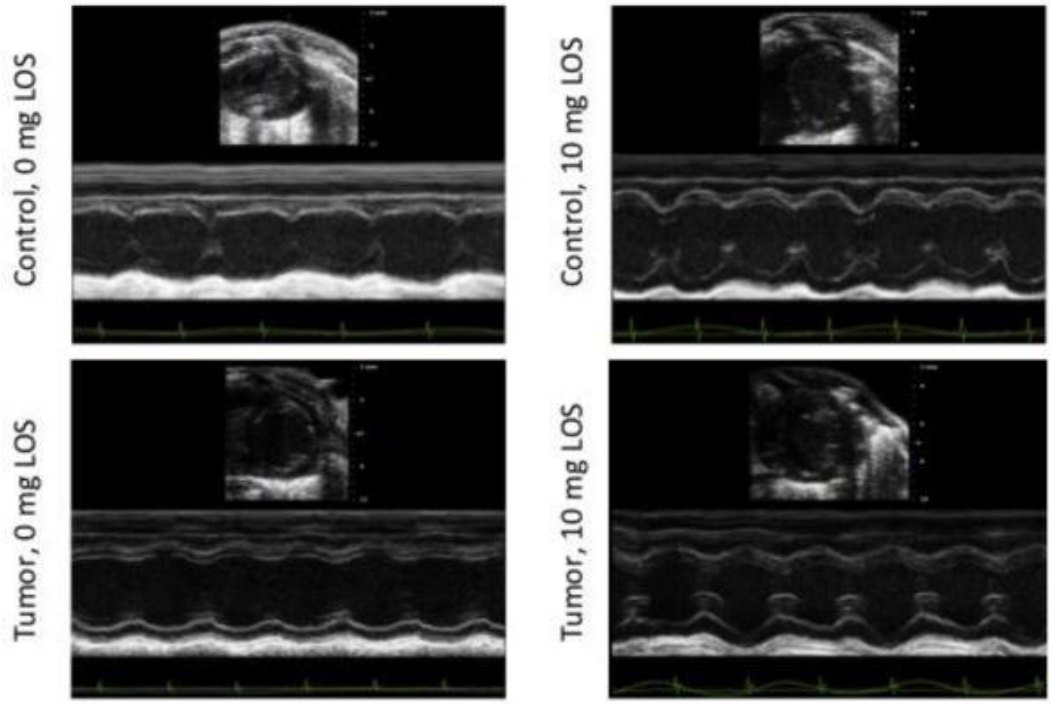

Figure 3. Representative M-mode *in vivo* echocardiographic images obtained at the mid-papillary muscle level of tumor-bearing and Losartan-treated mice. Images include electrocardiogram and respiratory traces at the bottom.

Tumor-induced cardiomyocyte dysfunction is improved with Losartan treatment

Percent sarcomeric peak shortening (%PS, the cellular equivalent of *in vivo* fractional shortening) (Figure 4A) was not affected by either tumor cell injection or Losartan treatment. However, time-to-90% peak shortening (TPS90) and time-to-90 percent relengthening (TR90) were significantly increased in tumor/sham compared to control/sham treated mice and further increased in tumor/LOS compared to tumor/sham treated mice. Statistical analyses indicated effects of tumor cell injection on TPS90 ($p<.0001$) and TR90

(p<0.05), and effects of Losartan treatment on TPS90 (p<.001) and TR90 (p<0.05). These data suggest that the effects of Losartan treatment on peak shortening and relengthening were independent of the tumor condition and could be related to the tendency of Losartan to cause hypertrophy.[27,28]

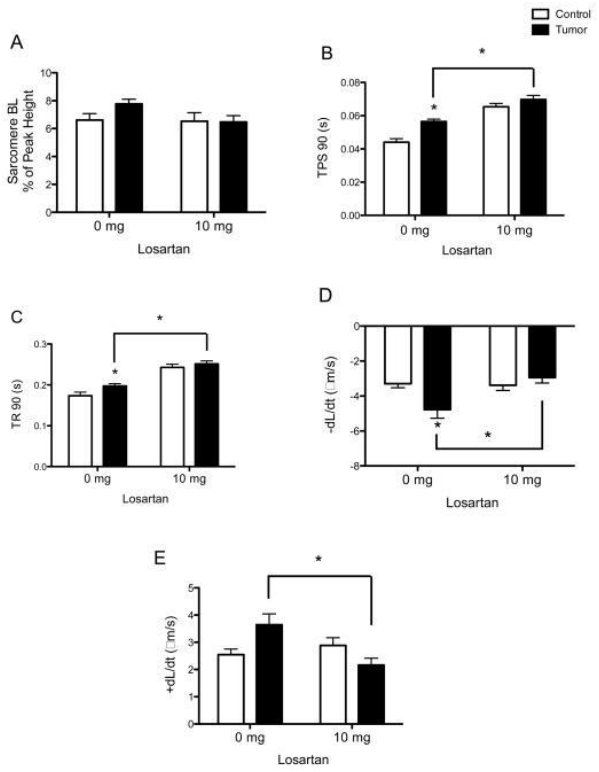

Figure 4. In vivo myocyte function in tumor-bearing and Losartan-treated mice. A, percent peak sarcomere shortening (Sarcomere BL). B, time to 90 percent of peak shortening (TPS90). C, time to 90 percent relengthening (TR90). D, velocity of myocyte shortening. E, velocity of myocyte relengthening. Data were analyzed using two-way ANOVA (tumor growth and Losartan treatment) and Bonferroni post hoc pairwise comparisons. * p<0.05 compared to respective control. Myocyte cell numbers: n=70 cells/12 mice control/sham, n=97 cells/17 mice tumor/sham, n=45 cells/4 mice control/LOS, n=61 cells/8 mice tumor/LOS.

In contrast, depolarization velocity (-dL/dt) was increased in tumor/sham compared to control/sham and tumor/LOS treated mice. Statistical analyses indicated an effect of Losartan treatment (p<0.001) and an interaction between tumor cell injection and Losartan treatment (p<0.005) on -dL/dt. The velocity of relengthening (+dL/dt) was significantly increased in tumor/sham compared to tumor/LOS mice. Statistical analyses indicated an interaction of tumor cell injection and Losartan treatment on +dL/dt (p<0.01) (Figures 4D

& E). These findings suggest an effect of Losartan on the mechanics of sarcomeric function that requires further mechanistic investigation.

Losartan treatment attenuated tumor-induced changes in calcium signaling

Calcium transient amplitude and calcium reuptake velocity were increased in tumor/sham compared to control/sham and tumor/LOS mice. Furthermore, calcium transient amplitude was increased in tumor/LOS but maximum velocity of calcium transients was not different compared to control/LOS treated mice. Statistical analyses revealed effects of tumor cell injection and Losartan treatment on calcium transient amplitude ($p<.001$), and an additional interaction effect of tumor cell injection and Losartan treatment on calcium reuptake velocity ($p<.001$) (Figure 5A–B). These effects on calcium transients and reuptake suggest that Losartan treatment normalized calcium currents in the myocytes of tumor-bearing mice.

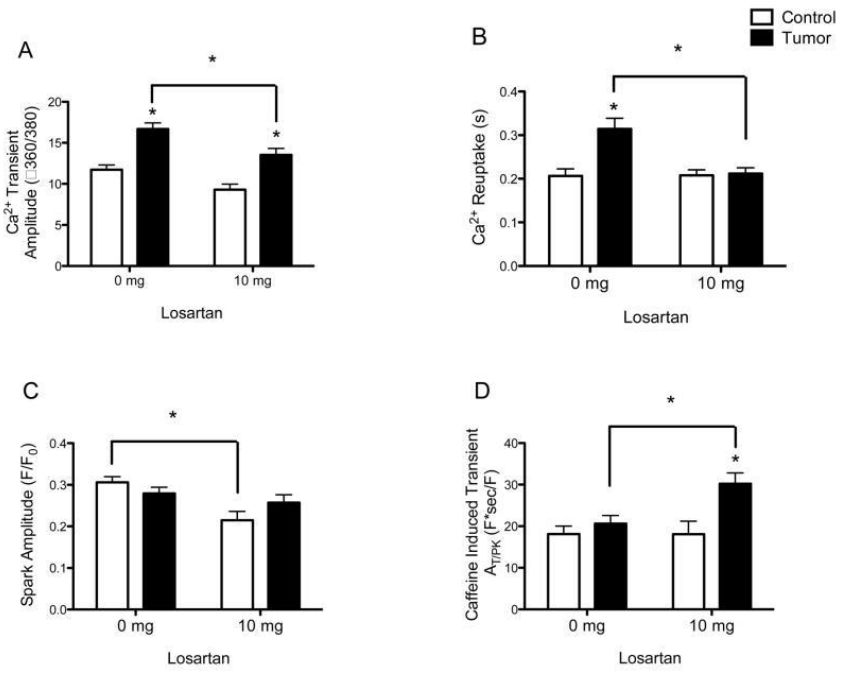

Figure 5. Cardiomyocyte calcium signaling in tumor-bearing and Losartan-treated mice. A, amplitude of stimulated Ca^{2+} transients. B, amplitude of calcium sparks. C, amplitude of caffeine induced Ca^{2+} release. D, Integration under the caffeine-induced Ca^{2+} release curve as an index of SR Ca^{2+} concentration. Data analyzed using two-way ANOVA (tumor growth, Losartan treatment), followed by Bonferroni post hoc pairwise comparisons. * $p<0.05$ compared to respective control. Myocyte cell numbers for calcium analysis:

Journal of Molecular and Cellular Cardiology, Vol 85 (August 2015): pg. 37-47. DOI.

n=27 cells/11 mice control/sham, n=40 cells/14 mice tumor/sham, n=29 cells/4 mice control/LOS, n=52 cells/8 mice tumor/LOS.

Spark amplitude was lower in control/LOS compared to control/sham treated mice. Statistical analyses indicated an effect of Losartan on spark amplitude ($p<0.01$) (Figure 5C). Caffeine-induced calcium release was increased in tumor/LOS compared to control/LOS and tumor/sham treated mice. Statistical analyses indicated an effect of tumor cell injection on caffeine induced calcium release ($p<0.005$) (Figure 5D).

GSH/GSSG levels are increased in hearts of tumor-bearing mice

Left ventricular GSH/GSSG levels were not different between groups; however, statistical analysis indicated an effect of tumor cell injection ($p<0.05$) on the GSH/GSSG ratio (Figure 6).

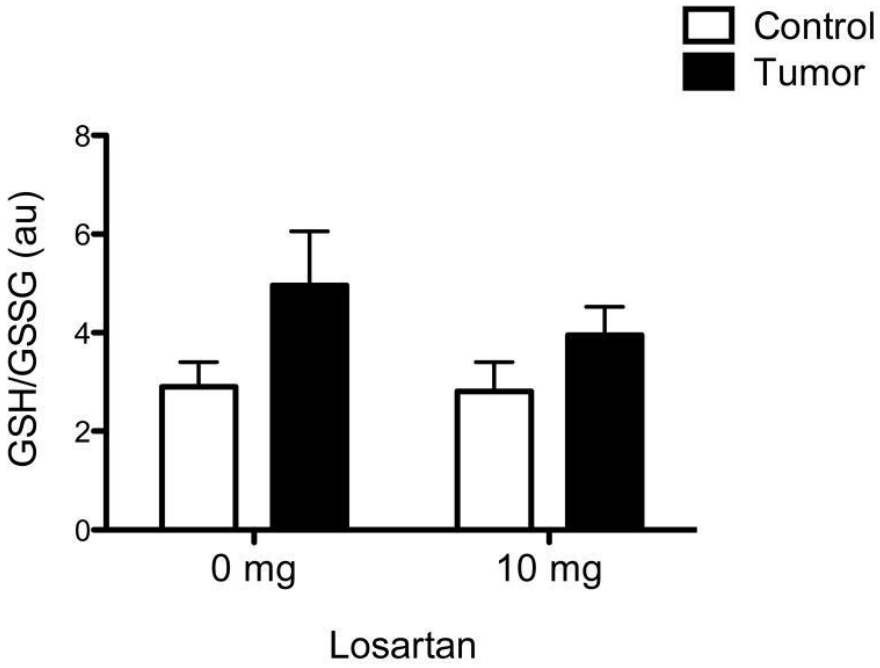

Figure 6. Oxidative stress in ventricular tissue of tumor-bearing and Losartan-treated mice. The ratio of GSH/GSSG was used to approximate oxidative stress in left ventricular tissue. Data analyzed using two-way ANOVA (tumor growth, Losartan treatment), followed by Bonferroni post hoc pairwise comparisons. No significance was observed with Losartan treatment. n=5.

Journal of Molecular and Cellular Cardiology, Vol 85 (August 2015): pg. 37-47. DOI.

Tumor growth and Losartan treatment affected blood pressure

Systolic blood pressure was lower in control/LOS compared to control/sham treated mice 12 days after tumor cell injection (data not shown). Statistical analyses indicated effects of Losartan treatment ($p<0.05$) and an interaction between Losartan treatment and tumor cell injection ($p<0.05$) on systolic blood pressure. Diastolic blood pressures and developed pressures were not different between groups 12 days after tumor cell injection and/or Losartan treatment. However, 18 days post tumor cell injection systolic and developed pressures were significantly lower in tumor/sham compared to control/sham mice. However, there was no difference in tumor/LOS treated mice compared to control/sham or control/LOS treated mice. Statistical analyses indicated interaction effects of tumor cell injection and Losartan treatment on systolic ($p<0.05$) and developed ($p<0.001$) blood pressures. Furthermore, diastolic blood pressures were lower in control/LOS and tumor/LOS treated mice compared to respective control/sham and tumor/LOS treated mice. Statistical analyses indicated an effect of Losartan treatment on diastolic blood pressure ($P<0.05$) (Table 3).

Table 3. Blood pressure in tumor-bearing and Losartan-treated mice. Systolic blood pressure, diastolic blood pressure and developed pressure on days 12 and 18. days after tumor cell injection. Data were analyzed using two-way ANOVA (tumor growth and Losartan treatment) and Bonferroni post hoc tests.

	control/sham (n=4)	**tumor/sham (n=4)**	**control/LOS (n=5)**	**tumor/LOS (n=5)**
D12 Systolic blood pressure (mmHg)	120±1	106±2	103±4	107±4
D12 Diastolic blood pressure (mmHg)	46±4	53±5	46±4	53±10
D12 developed pressure (mmHg)	74±3	54±6	58±6	55±10
D18 Systolic blood pressure (mmHg)	125±4	99±3*	103±3	109±9
D18 Diastolic blood pressure (mmHg)	58±4	59±7	41±3	41±2
D18 developed pressure (mmHg)	68±7	40±6*	61±2	68±7

*$p<0.05$ compared to respective control.

Journal of Molecular and Cellular Cardiology, Vol 85 (August 2015): pg. 37-47. DOI.

Tumor cell injection increased Angiotensin II serum levels

Angiotensin II serum levels from tumor/control and tumor/LOS treated mice were increased compared to sham/control and sham/LOS treated mice, respectively. Statistical analyses indicated a significant effect of tumor cell injection on Angiotensin II serum levels (Figure 7).

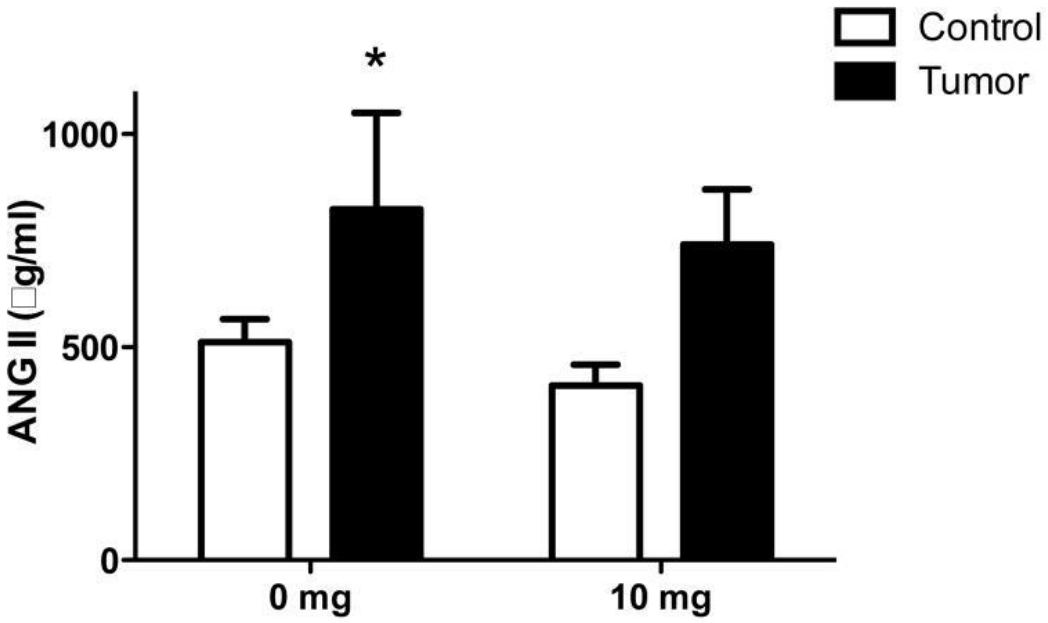

Figure 7. Angiotensin II Protein levels in mouse serum of tumor-bearing and Losartan treated mice 18 days after tumor cell or sham injection. Data were analyzed using two-way ANOVA (tumor growth, Losartan treatment), followed by Bonferroni post hoc pairwise comparisons. * $p<0.01$ compared to control, n=4.

Inhibitory effects of Losartan on c26 Adenocarcinoma cell proliferation

Losartan treatment significantly inhibited the proliferation of c26 adenocarcinoma cells *in vitro* compared to non-Losartan treated control cells ($p<0.001$) (Figure 8).

Journal of Molecular and Cellular Cardiology, Vol 85 (August 2015): pg. 37-47. DOI.

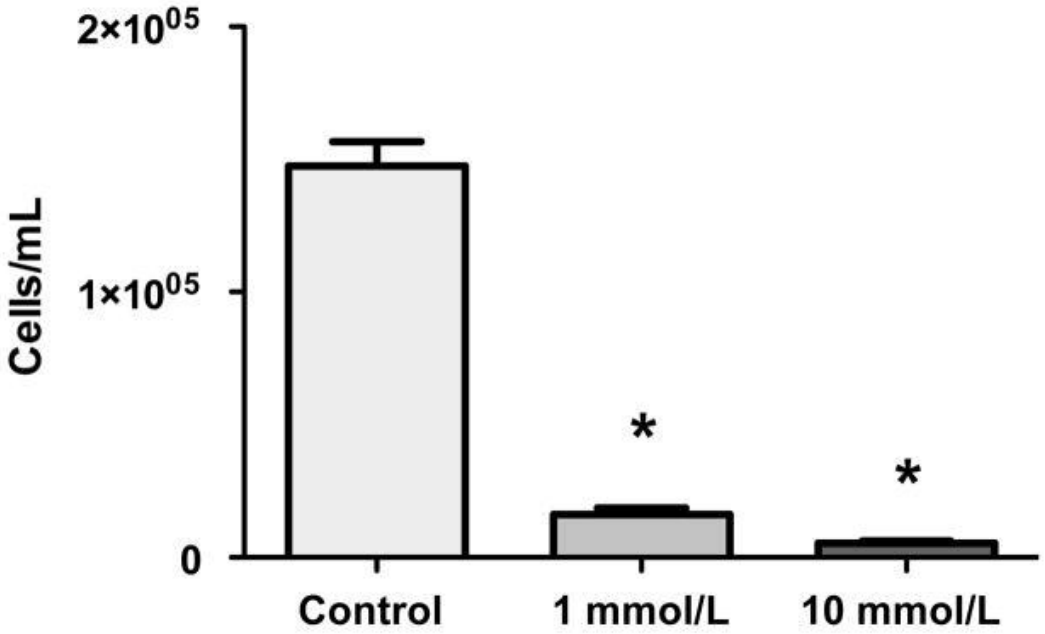

Figure 8. Effects of Losartan on c26 Adenocarcinoma cell proliferation. Cells were cultured with 1 mM/L, 10 mM/L or without Losartan for 3 days. Data were analyzed using one-way ANOVA. Losartan significantly inhibited the proliferation of c26 Adenocarcinoma cell at both concentrations. $p<0.001$, $n=6$.

Discussion

As shown in Table 1, treatment with Losartan preserved gastrocnemius muscle mass in c26 tumor-bearing mice, without improving body weight. The RAAS affects fatty acid and glucose metabolism and ACE deficiency, resulting in a reduction in body weight.[29] Based on these data, we speculate that the observed reduction in body weight of tumor-bearing and Losartan treated mice could be related to Losartan-induced alterations of the RAAS and subsequent effects on glucose and fatty acid metabolism. Tumor bearing and Losartan treatment had no significant effects on heart weight normalized to body weight. Based on the results of others, however, it is likely that heart mass may have decreased had the tumor-bearing mice been allowed to develop more severe cachexia prior to euthanasia and the presented results are not due to cachexia but tumor presence.[5]

Echocardiographic studies confirmed our earlier findings of systolic dysfunction in c26 tumor-bearing mice[3] (Table 2). This dysfunction was attenuated by treatment with Losartan. These data

are in accordance with others that investigated in liver cancer induced cardiac failure and reported an attenuation of tumor induced left ventricular dysfunction in beta blocker and mineralocorticoid receptor antagonist treated mice.[10] Our data suggest that Losartan may be useful in preserving myocardial function in patients with cancer associated cardiac dysfunction.

Tumor cell injection prolonged contraction and depolarization velocities of isolated cardiomyocytes. At the cellular level, tumor progression prolonged TPS90 and TR90 in isolated cardiomyocytes. However, Losartan treatment also prolonged TPS90 and TR90 in myocytes from tumor and control mice, such that there were no longer any differences between the myocytes of tumor and control mice (Figures 4B and 4C). These data suggest that other non-myocyte cell types could play a role in normalization of myocardial function in the tumor-bearing mice, such as activation of proteins involved in the production of the extracellular matrix. Other possible explanations for the improvements in *in vivo* cardiac function, but not *in vitro* cellular parameters, include myocyte apoptosis or a change in intracellular communication.

We also examined the direct effects of Losartan treatment on blood pressure. Our results show a reduction of systolic blood pressure and developed pressure, representing the circulatory consequences and confirming the reported *in vitro* and *in vivo* results indicating myocardial dysfunction 18 days following tumor cell injection. Distinctly, Losartan affected blood pressure in the presence as well as the absence of tumor, suggesting direct effects of Losartan on blood pressure. The reduction in blood pressure indicates a direct effect of Losartan on the circulation (Table 3).

It is clear that Losartan improved myocardial function in this mouse model of cancer cachexia and there are several plausible mechanisms. Our data indicate that Losartan altered pro-inflammatory activity as observed by a decrease in IL-6 mRNA expression in the heart, which is thought to be a key step in activation of the UPP of myosin degradation.[30] Activation of the UPP is a known effect of AngII1[6] and pro-inflammatory cytokines, such as IL-1, IL-6, and TNF-α induced NF-κB activation have been reported to be the mechanisms of altered striated muscle mass in tumor-bearing cancer models,[31] thus it

is not surprising that Losartan treatment would preserve gastrocnemius muscle mass in tumor-bearing mice (Table 1).

Losartan treatment affected Ca^{2+} transient amplitude in cardiomyocytes from both the control and tumor groups (Figure 5A), but affected the area under the Ca^{2+} release curve (Figure 5D), which is an index of SR Ca^{2+} levels, in only the tumor-bearing mice. The change in the caffeine-induced Ca^{2+} release curve was potentially due to Losartan increasing the expression of NCX,[32] which is the sole channel responsible for clearing Ca^{2+} from the cytosol during treatment with caffeine. It is, however, unlikely that Ca^{2+} signaling is the entire mechanism of improvement following Losartan treatment as tumor-induced changes in the amplitude of the Ca^{2+} transient are unaffected by Losartan. However, these data require further investigation.

The increase in the relative amount of MHC-β is consistent with an earlier report[5] from a study using the same tumor-bearing model. The increased amount of MHC-β in the tumor-bearing mice likely contributed to the observed prolonged time to peak shortening in isolated myocytes. Even small differences in the MHC isoform composition of isolated cardiomyocytes can affect power output, with an increase in the amount of MHC-β being associated with reduced power.[33–35] However, an increase in the amount of MHC-β is associated with increased economy of myocardial contraction,[36] potentially providing a beneficial adaptation in the tumor-bearing mice, which eventually develop a reduction in cardiac wall thickness.[2] The increase in the amount of MHC-β was also associated with an increase in the amount of one of the apparent MHC-α fragments (MHC-α') in tumor-bearing, which could also be an adaptation to maintain force generating ability with increased economy. Interestingly, increased MHC breakdown has also been reported in skeletal muscle with the same tumor-bearing mouse model.[37]

The relative amount of MHC-β was not different between control/LOS and tumor/LOS mice. This is consistent with Losartan reversing the increase in the mRNA and protein levels of MHC-β following induced heart failure in rats.[38–40] There was an increase in the relative amount of apparent MHC-α proteolytic fragments in Losartan-treated mice. The responsible mechanism is not known, but it

is possible that there is increased proteolytic activity associated with changes in MHC expression and replacement in myofibrils during Losartan treatment.

Ca^{2+} transient amplitude was altered in tumor/LOS mice (Figure 5A), with no change in cardiomyocyte peak shortening (Figure 4A). This suggests that there could have been a change in myofilament Ca^{2+} sensitivity, which is often observed during ventricular hypertrophy.[41] This would also be a potential explanation for the decrease in myocardial function in the tumor-bearing mice.

AngII is known to increase ROS production in various diseases.[42–44] AngII causes the formation of reactive oxygen species in vivo, mediated by AT_2 in response to hypertension. Thus, we also examined the GSH/GSSG ratios as a marker for the presence of oxidative stress in heart tissue as a potential mechanism of myocardial dysfunction observed in tumor-bearing mice. While tumor presence did increase overall GSH/GSSG levels in heart tissue, Losartan treatment surprisingly had no effect on production of this particular marker of oxidative stress (Figure 6). AngII receptor blockers have been shown to reduce the production of ROS in the kidneys in a mouse model of hypertension-induced cardiomyopathy. Based on these reports, our data suggest that the observed improvement of cardiac function could be related to the direct effects of other reactive oxygen species or hormone related improvement in blood pressure. AngII is not likely to be involved in the direct cardiac mechanism of action for Losartan-mediated improvements in myocardial function in tumor-bearing mice.

Losartan is a selective AT_1 receptor antagonist without serious adverse effects that is commonly used for the treatment of hypertension. In our model Losartan treatment reduced diastolic blood pressure in control and tumor mice, but prevented tumor associated reduction in systolic blood pressure and most importantly developed pressure.

Accumulating evidence supports the notation that the RAAS directly impacts tumor progression through tumor cell proliferation and tumor angiogenesis. Furthermore, Losartan has been shown to improve the effects of chemotherapeutics, potentially through an enhancement of drug delivery in breast and pancreatic cancer

models.[45] Therefore, another plausible explanation for the observed Losartan associated prevention of tumor-associated development of cardiac dysfunction could be linked to direct effects of Losartan on tumor cells and the tumor itself. However, the direct impact of Losartan on adenocarcinoma cell proliferation has not been investigated. Thus, we examined the effects of Losartan on c26 adenocarcinoma cells proliferation and tumor progression. Our data indicated that Losartan treatment impaired c26 adenocarcinoma cell proliferation *in vitro* and reduced tumor weight *in vivo*. In summary, our *in vitro* data indicate a direct effect of Losartan on tumor cells, reducing c26 tumor cell proliferation. Antagonizing the AT_1 receptor by Losartan treatment could be a potential mechanism for the herein reported reduction in tumor progression and subsequent prevention of tumor associated development of cardiac dysfunction.

Taken together, our data indicate that Losartan treatment impaired c26 adenocarcinoma cell proliferation *in vitro*, reduced tumor weight *in vivo*, prevented the expression of in cardiac degeneration and inflammation involved mediators and attenuated the development of tumor-associated cardiac dysfunction *in vivo* and *in vitro*. Losartan has been shown to reduce VEGF concentrations in various models, which subsequently impairs vascular formation in neoplastic tissue affecting tumor presence. In our c26 adenocarcinoma model Losartan treatment reduced tumor weight and improved tumor induced cardiac dysfunction and our *in vitro* data suggest, that the reduction in tumor weight may be due to Losartan induced reduction in c26 adenocarcinoma cell proliferation. However, one limitation of our study is that the presented data do not indicate if the beneficial effects of Losartan on tumor-induced cardiac dysfunction are based on direct effects of Losartan on tumor cells or the prevention of tumor progression and secondary to the heart. Hence, we cannot rule out primary effects of Losartan to the heart that directly prevent the development of tumor-induced cardiac dysfunction.

Our herein presented results provide promising new insights into the potential role for Losartan, a widely used AT_1 receptor antagonist that has no serious side effects, for the treatment of tumor-induced myocardial dysfunction in cancer patients.

Journal of Molecular and Cellular Cardiology, Vol 85 (August 2015): pg. 37-47. DOI.

Highlights

- Losartan treatment has a beneficial effect on tumor-mediated cardiac dysfunction.
- Reactive oxygen species are a key component of cancer-mediated cardiac dysfunction.
- Treatment with Losartan affects tumor cell growth in vitro.

Supplementary Material

Material and Methods

Assessment of MHC Isoform Composition. Left ventricular homogenates were prepared from the hearts of control and c26 tumor-bearing mice, as in Reiser and Kline [1]. Myosin heavy chain (MHC) isoform composition of left ventricular homogenates was examined using SDS-PAGE and scanning densitometry. Gels were also run for mass spectrometry and immunoblotting. Separating gels consisted of 7% acrylamide, with a 50:1 acrylamide:bis-acrylamide crosslinking ratio, and 5% (v/v) glycerol. Additional details for the separating and stacking gels were as described in Reiser and Kline [1]. The gels were run for 21 hours at 8°C and 230 constant volts. Silver-staining and scanning of the gels were as described previously [1, 2], except that the gels were scanned before drying. One gel was stained with Coomassie Blue and bands were excised and analyzed with liquid chromatography, coupled to tandem mass spectrometry, in the Campus Chemical Instrument Center at The Ohio State University [3]. Another gel was used for immunoblotting that was probed with an MF 20 antibody, which recognizes all sarcomeric MHC isoforms (supernatant from the Developmental Studies Hybridoma Bank was diluted to 1:50). Protein bands were detected with a secondary antibody conjugated with alkaline phosphatase, as previously described [4].

Results

Changes in MHC Isoforms: The amounts of MHC-α and MHC-β were determined by densitometry of silver-stained gels (example shown in panel A of Figure S1). There was a small, but significantly ($P<0.005$) greater amount of MHC-β, relative to the total amount of MHC, in the left ventricle of tumor-bearing mice, compared to control mice. There was no difference in the relative amount of MHC-β between control/LOS and tumor/LOS mice. Several protein bands, with electrophoretic mobilities that were greater than that of MHC isoforms, were observed on the same gel. An immunoblot with an antibody that recognizes all sarcomeric MHC isoforms (MF 20, supernatant, diluted 1:50, Developmental studies Hybridoma Bank, University of Iowa, Iowa City, IA) was run and three prominent bands were detected, corresponding to MHC-α, MHC-β and a band with greater mobility (panel C of Figure S1). The latter band and another band, with even greater mobility and

which was not suffucently abundant to be detected by the antibody but was visible on stained gels, were excised from a Coomassie-stained gel. These bands were submitted for analysis by mass spectrometry in the Ohio State University Campus Chemical Instrument Center.

The six peptides from the digestion of both excised bands that had the strongest matches with MHC-α were the same for both bands. The MOWSE scores from mass spectrometry were 8227 and 2975 for MHC-α′ and MHC-α″, respectively. These scores far exceed the score (i.e., 53) that is associated with a significant probability of correct identification. Given the high MOWSE scores, we conclude that these bands are likely to be proteolytic fragments of MHC-α and are labeled as MHC-α′ and MHC-α″. The relative amounts of MHC-α′ and MHC-α″ were individually quantitated relative to the total MHC-α pool (i.e., the sum of MHCα + MHC-α′ + MHC-α″) in each sample. The relative amount of MHC-α′ was significantly greater in tumor-bearing mice, compared to control mice, both with and without Losartan treatment. Losartan treatment did not affect the relative amount of MHC-α′ in control mice, but the relative amount of MHC-α′ was greater in tumor-bearing mice that were treated with Losartan, compared to untreated tumor-bearing mice. There was no difference in the relative amount of MHC-α″ between untreated control and tumor-bearing groups. Losartan treatment was associated with an increase in the relative amount of MHC-α″ in control mice, but not in tumor-bearing mice.

Figure

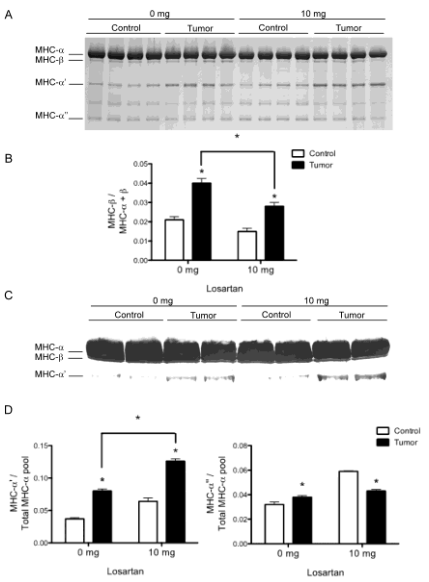

Figure. S1. Cardiac myosin heavy chain (MHC) isoforms and proteolytic fragments in control and tumor-bearing mice. The MHC region of an SDS gel loaded with left ventricular samples from control and tumor-bearing mice, with or without Losartan treatments. B, quantitation of the amount of MHC-β, relative to total intact MHC (MHC-α + MHC-β), from scanning densitometry of silver-stained gels and quantitation of the amounts of two proteolytic fragments of MHC-α (MHC-α′ and MHC-α″), relative to the total MHC-α pool (MHC-α + MHC-α′ + MHC-α″), from scanning densitometry of silver-stained gels. * $p<0.05$ compared to respective control (n=6).

Journal of Molecular and Cellular Cardiology, Vol 85 (August 2015): pg. 37-47. DOI.

References

[1] Reiser PJ, Kline WO. Electrophoretic separation and quantitation of cardiac myosin heavy chain isoforms in eight mammalian species. *The American journal of physiology*. 1998;274:H1048-53.
[2] Blough ER, Rennie ER, Zhang F, Reiser PJ. Enhanced electrophoretic separation and resolution of myosin heavy chains in mammalian and avian skeletal muscles. *Analytical biochemistry*. 1996;233:31-5.
[3] Reiser PJ, Bicer S. Multiple isoforms of myosin light chain 1 in pig diaphragm slow fibers: correlation with maximal shortening velocity and force generation. *Archives of biochemistry and biophysics*. 2006;456:112-8.
[4] Bergrin M, Bicer S, Lucas CA, Reiser PJ. Three-dimensional compartmentalization of myosin heavy chain and myosin light chain isoforms in dog thyroarytenoid muscle. *American journal of physiology Cell physiology*. 2006;290:C1446-58.

Acknowledgments

Funding

The work was supported by the National Institutes of Health [NR012618 to DOM/LEW/PJR and #ES019923 to LEW].

The authors would like to thank Dr. Mary Cismowski from the Center for Cardiovascular and Pulmonary Research at the Research Institute of Nationwide Children's Hospital for performing the GSH/GSSG assays. The MF 20 monoclonal antibody, developed by Dr. Donald A. Fischman, Cornell University, was obtained from the Developmental Studies Hybridoma Bank, created by the NICHD of the NIH and maintained at The University of Iowa, Department of Biology, Iowa City, IA 52242. Tail cuff blood pressure studies were conducted with the guidance of Dr. Cameron Rink and Ms. Hallie Harris from the Ohio State University.

References

1. Douglas E, McMillan DC. Towards a simple objective framework for the investigation and treatment of cancer cachexia: The Glasgow Prognostic Score. *Cancer treatment reviews*. 2014;40:685–91.
2. Tian M, Asp ML, Nishijima Y, Belury MA. Evidence for cardiac atrophic remodeling in cancer-induced cachexia in mice. *International journal of oncology*. 2011;39:1321–6.
3. Xu H, Crawford D, Hutchinson KR, Youtz DJ, Lucchesi PA, Velten M, et al. Myocardial dysfunction in an animal model of cancer cachexia. *Life sciences*. 2011;88:406–10.
4. Zuppinger C, Timolati F, Suter TM. Pathophysiology and diagnosis of cancer drug induced cardiomyopathy. *Cardiovascular toxicology*. 2007;7:61–6.
5. Tian M, Nishijima Y, Asp ML, Stout MB, Reiser PJ, Belury MA. Cardiac alterations in cancer-induced cachexia in mice. *International journal of oncology*. 2010;37:347–53.
6. Tamarat R, Silvestre JS, Durie M, Levy BI. Angiotensin II angiogenic effect in vivo involves vascular endothelial growth factor- and inflammation-related pathways. *Laboratory investigation; a journal of technical methods and pathology*. 2002;82:747–56.
7. Chauhan VP, Stylianopoulos T, Martin JD, Popovic Z, Chen O, Kamoun WS, et al. Normalization of tumour blood vessels improves the delivery of nanomedicines in a size-dependent manner. *Nature nanotechnology*. 2012;7:383–8.
8. Bosch X, Rovira M, Sitges M, Domenech A, Ortiz-Perez JT, de Caralt TM, et al. Enalapril and carvedilol for preventing chemotherapy-induced left ventricular systolic dysfunction in patients with malignant hemopathies: the OVERCOME trial (preventiOn of left Ventricular dysfunction with Enalapril and caRvedilol in patients submitted to intensive ChemOtherapy for the treatment of Malignant hEmopathies) *Journal of the American College of Cardiology*. 2013;61:2355–62.
9. Cardinale D, Colombo A, Sandri MT, Lamantia G, Colombo N, Civelli M, et al. Prevention of high-dose chemotherapy-induced cardiotoxicity in high-risk patients by angiotensin-converting enzyme inhibition. *Circulation*. 2006;114:2474–81.
10. Springer J, Tschirner A, Haghikia A, von Haehling S, Lal H, Grzesiak A, et al. Prevention of liver cancer cachexia-induced cardiac wasting and heart failure. *European heart journal*. 2014;35:932–41.
11. Kim S, Toyokawa H, Yamao J, Satoi S, Yanagimoto H, Yamamoto T, et al. Antitumor effect of angiotensin II type 1 receptor blocker losartan for orthotopic rat pancreatic adenocarcinoma. *Pancreas*. 2014;43:886–90.

12. Brink M, Price SR, Chrast J, Bailey JL, Anwar A, Mitch WE, et al. Angiotensin II induces skeletal muscle wasting through enhanced protein degradation and down-regulates autocrine insulin-like growth factor I. *Endocrinology*. 2001;142:1489–96.
13. Brink M, Wellen J, Delafontaine P. Angiotensin II causes weight loss and decreases circulating insulin-like growth factor I in rats through a pressor-independent mechanism. *The Journal of clinical investigation*. 1996;97:2509–16.
14. Semprun-Prieto LC, Sukhanov S, Yoshida T, Rezk BM, Gonzalez-Villalobos RA, Vaughn C, et al. Angiotensin II induced catabolic effect and muscle atrophy are redox dependent. *Biochemical and biophysical research communications*. 2011;409:217–21.
15. Sukhanov S, Semprun-Prieto L, Yoshida T, Michael Tabony A, Higashi Y, Galvez S, et al. Angiotensin II, oxidative stress and skeletal muscle wasting. *The American journal of the medical sciences*. 2011;342:143–7.
16. Sanders PM, Russell ST, Tisdale MJ. Angiotensin II directly induces muscle protein catabolism through the ubiquitin-proteasome proteolytic pathway and may play a role in cancer cachexia. *British journal of cancer*. 2005;93:425–34.
17. Murphy KT, Chee A, Trieu J, Naim T, Lynch GS. Inhibition of the renin-angiotensin system improves physiological outcomes in mice with mild or severe cancer cachexia. *International journal of cancer Journal international du cancer*. 2013;133:1234–46.
18. Wold LE, Ying Z, Hutchinson KR, Velten M, Gorr MW, Velten C, et al. Cardiovascular remodeling in response to long-term exposure to fine particulate matter air pollution. *Circulation Heart failure*. 2012;5:452–61.
19. Pombo JF, Troy BL, Russell RO., Jr Left ventricular volumes and ejection fraction by echocardiography. *Circulation*. 1971;43:480–90.
20. Monreal G, Nicholson LM, Han B, Joshi MS, Phillips AB, Wold LE, et al. Cytoskeletal remodeling of desmin is a more accurate measure of cardiac dysfunction than fibrosis or myocyte hypertrophy. *Life sciences*. 2008;83:786–94.
21. Ren J, Wold LE, Epstein PN. Diabetes enhances acetaldehyde-induced depression of cardiac myocyte contraction. *Biochemical and biophysical research communications*. 2000;269:697–703.
22. Wold LE, Aberle NS, 2nd, Ren J. Doxorubicin induces cardiomyocyte dysfunction via a p38 MAP kinase-dependent oxidative stress mechanism. *Cancer detection and prevention*. 2005;29:294–9.
23. Wold LE, Ceylan-Isik AF, Fang CX, Yang X, Li SY, Sreejayan N, et al. Metallothionein alleviates cardiac dysfunction in streptozotocin-induced diabetes: role of Ca2+ cycling proteins, NADPH oxidase, poly(ADP-

Ribose) polymerase and myosin heavy chain isozyme. *Free radical biology & medicine*. 2006;40:1419–29.
24. Sheehan KA, Zima AV, Blatter LA. Regional differences in spontaneous Ca2+ spark activity and regulation in cat atrial myocytes. *The Journal of physiology.* 2006;572:799–809.
25. Kode A, Rajendrasozhan S, Caito S, Yang SR, Megson IL, Rahman I. Resveratrol induces glutathione synthesis by activation of Nrf2 and protects against cigarette smoke-mediated oxidative stress in human lung epithelial cells. *American journal of physiology Lung cellular and molecular physiology.* 2008;294:L478–88.
26. Chen X, Meng Q, Zhao Y, Liu M, Li D, Yang Y, et al. Angiotensin II type 1 receptor antagonists inhibit cell proliferation and angiogenesis in breast cancer. *Cancer letters*. 2013;328:318–24.
27. Zou Y, Lin L, Ye Y, Wei J, Zhou N, Liang Y, et al. Qiliqiangxin inhibits the development of cardiac hypertrophy, remodeling, and dysfunction during 4 weeks of pressure overload in mice. *Journal of cardiovascular pharmacology.* 2012;59:268–80.
28. Liu Y, Leri A, Li B, Wang X, Cheng W, Kajstura J, et al. Angiotensin II stimulation in vitro induces hypertrophy of normal and postinfarcted ventricular myocytes. *Circulation research*. 1998;82:1145–59.
29. Jayasooriya AP, Mathai ML, Walker LL, Begg DP, Denton DA, Cameron-Smith D, et al. Mice lacking angiotensin-converting enzyme have increased energy expenditure, with reduced fat mass and improved glucose clearance. *Proceedings of the National Academy of Sciences of the United States of America*. 2008;105:6531–6.
30. Fu D, Ma Y, Wu W, Zhu X, Jia C, Zhao Q, et al. Cell-cycle-dependent PC-PLC regulation by APC/C(Cdc20)-mediated ubiquitin-proteasome pathway. *Journal of cellular biochemistry*. 2009;107:686–96.
31. Wysong A, Couch M, Shadfar S, Li L, Rodriguez JE, Asher S, et al. NF-kappaB inhibition protects against tumor-induced cardiac atrophy in vivo. *The American journal of pathology*. 2011;178:1059–68. [
32. Ferreira JC, Moreira JB, Campos JC, Pereira MG, Mattos KC, Coelho MA, et al. Angiotensin receptor blockade improves the net balance of cardiac Ca(2+) handling-related proteins in sympathetic hyperactivity-induced heart failure. *Life sciences*. 2011;88:578–85.
33. Herron TJ, Korte FS, McDonald KS. Loaded shortening and power output in cardiac myocytes are dependent on myosin heavy chain isoform expression. *American journal of physiology Heart and circulatory physiology.* 2001;281:H1217–22.
34. Herron TJ, McDonald KS. Small amounts of alpha-myosin heavy chain isoform expression significantly increase power output of rat cardiac myocyte fragments. *Circulation research*. 2002;90:1150–2.

35. Korte FS, Herron TJ, Rovetto MJ, McDonald KS. Power output is linearly related to MyHC content in rat skinned myocytes and isolated working hearts. *American journal of physiology Heart and circulatory physiology.* 2005;289:H801–12.
36. Belus A, Piroddi N, Ferrantini C, Tesi C, Cazorla O, Toniolo L, et al. Effects of chronic atrial fibrillation on active and passive force generation in human atrial myofibrils. *Circulation research*. 2010;107:144–52.
37. Acharyya S, Ladner KJ, Nelsen LL, Damrauer J, Reiser PJ, Swoap S, et al. Cancer cachexia is regulated by selective targeting of skeletal muscle gene products. *The Journal of clinical investigation*. 2004;114:370–8.
38. Pourdjabbar A, Parker TG, Nguyen QT, Desjardins JF, Lapointe N, Tsoporis JN, et al. Effects of pre-, peri-, and postmyocardial infarction treatment with losartan in rats: effect of dose on survival, ventricular arrhythmias, function, and remodeling. *American journal of physiology Heart and circulatory physiology.* 2005;288:H1997–2005.
39. Wellner M, Dechend R, Park JK, Shagdarsuren E, Al-Saadi N, Kirsch T, et al. Cardiac gene expression profile in rats with terminal heart failure and cachexia. *Physiological genomics*. 2005;20:256–67.
40. Babick A, Chapman D, Zieroth S, Elimban V, Dhalla NS. Reversal of subcellular remodelling by losartan in heart failure due to myocardial infarction. *Journal of cellular and molecular medicine*. 2012;16:2958–67.
41. Westfall MV, Borton AR, Albayya FP, Metzger JM. Myofilament calcium sensitivity and cardiac disease: insights from troponin I isoforms and mutants. *Circulation research*. 2002;91:525–31.
42. Wang G, Sarkar P, Peterson JR, Anrather J, Pierce JP, Moore JM, et al. COX-1-derived PGE2 and PGE2 type 1 receptors are vital for angiotensin II-induced formation of reactive oxygen species and Ca(2+) influx in the subfornical organ. *American journal of physiology Heart and circulatory physiology.* 2013;305:H1451–61.
43. Lee DY, Wauquier F, Eid AA, Roman LJ, Ghosh-Choudhury G, Khazim K, et al. Nox4 NADPH oxidase mediates peroxynitrite-dependent uncoupling of endothelial nitric-oxide synthase and fibronectin expression in response to angiotensin II: role of mitochondrial reactive oxygen species. *The Journal of biological chemistry*. 2013;288:28668–86.
44. Dikalov SI, Nazarewicz RR. Angiotensin II-induced production of mitochondrial reactive oxygen species: potential mechanisms and relevance for cardiovascular disease. *Antioxidants & redox signaling*. 2013;19:1085–94.
45. Chauhan VP, Martin JD, Liu H, Lacorre DA, Jain SR, Kozin SV, et al. Angiotensin inhibition enhances drug delivery and potentiates chemotherapy by decompressing tumour blood vessels. *Nature communications.* 2013;4:2516.